Journal of Engineering Research 12 (2024) 502–510

Contents lists available at ScienceDirect

Journal of Engineering Research

journal homepage: www.journals.elsevier.com/journal-of-engineering-research

Full length article

Microstructure, mechanical and tribological properties of Al/Cu functionally graded material fabricated through powder metallurgy

Vasavi Boggarapu[a,*], P.S. Rama Sreekanth[a,*], Venkateswara Babu Peddakondigalla[b]

[a] School of Mechanical Engineering, VIT-AP University, Amaravati, Andhra Pradesh, India
[b] Department of Mechanical Engineering, Vasireddy Venkatadri Institute of Technology, Guntur, India

ARTICLE INFO

Keywords:
Functionally graded material
Hardness
Compressive strength
Sliding wear
Coefficient of friction

ABSTRACT

Mechanical and tribological behavior of five layered Al/Cu functionally graded material (FGM) produced by powder metallurgy was presented in the study. Compressive strength and hardness was evaluated on Universal testing machine and Vickers hardness tester respectively. Tribological characteristics in terms of frictional coefficient and wear rate was examined on pin-on-disc tribometer under the influence of different normal loading, sliding velocity and sliding distance conditions. FGM showed varied hardness along the thickness direction and maximum hardness of 86 HV was found at graded region due to the formation of intermetallic compound ($CuAl_2$). Compressive strength of FGM was 40.9% and 22.7% greater than pure Al and pure Cu samples. Al/Cu FGM exhibited superior friction and wear characteristics over base materials. To understand the failure mechanisms on fracture and worn out surfaces, they were observed under Scanning Electron Microscopy (SEM).

Introduction

Functionally graded materials (FGMs) having inhomogeneous composition and properties to make them suitable for various engineering and industrial applications. Continuous change in microstructure, material composition and porosity results in gradation of mechanical and/or thermal properties from one surface to other. FGMs overcome the problems associated with composite laminates such as fiber delamination and matrix cracking [1–4]. Moreover, composites have low strength, toughness, and less wear resistance. Particularly, Aluminum (Al) based composites have limitations in certain applications like turbine blades, crank shafts, and aerospace structural components. As an alternative, Al based FGMs were developed to attain multiple properties in a single material. FGMs display variation in composition, density, grain size, and microstructure from their base materials [5,6]. Broad range of processing techniques have been employed to fabricate FGMs which were categorized as transport and constructive. Transportation techniques forms gradation in components due to diffusion of heat conduction, atomic and fluid flow. While constructive methods obtain gradients in stepwise (layer by layer) with controlled distribution of constituent elements [7,8]. Powder metallurgy (PM) is one among the widely used constructive processing methods to obtain stepped gradation. Adequate research was reported on development of FGMs through powder metallurgy process wherein gradients were obtained by changing the volume fraction of constituents from layer to layer. Cong et al. [9] fabricated 5 layered Al/Cu functionally graded material (FGM) using PM process with changing the volume fraction of copper. Authors have studied the variation in microstructure, material composition, and mechanical properties at individual layers. Xu et al. [10] studied the fatigue crack growth in Al/SiC FGM produced through PM. It was observed from their study that FGMs show superior crack resistance compared to metal matrix composites. Zhu et al. [11] prepared ZrO2/NiCr FGM with stepwise variation in zirconia content. The researchers concluded that FGMs can eliminate sharp interfaces with that of traditional metal-ceramic joints. Kwon et al. [12] developed four layered Al/CNT FGM containing 0–15 vol% of CNT filler particles. Increase in CNT content resulted in variation of Vickers hardness value from 30HV to 260HV. Similar behavior was observed with Al alloy/SiC FGM as reported by Gorkem et al. [13]. Al/alumina FGMs developed through powder metallurgy showed a decrement in density at individual layers after sintering process as reported by Farah et al. [14].

Aluminum found to be widely used matrix material for FGMs owing to its light weight and specific strength. But it possesses low tensile and impact strengths which was improved with the addition of metal or ceramic reinforcement particles [15,16]. Due to large variation in

* Corresponding authors.
E-mail addresses: boggarapu.vasavi7@gmail.com (V. Boggarapu), happyshrikanth@gmail.com (P.S. Rama Sreekanth).

https://doi.org/10.1016/j.jer.2023.100119
Received 27 April 2023; Received in revised form 8 June 2023; Accepted 15 June 2023

thermal properties, metal and ceramic functionally graded combination suffers high residual stresses. Thus, metal/ceramic FGMs were replaced with metal/metal FGMs to overcome these difficulties. In particular, aluminum-copper (Al/Cu) FGM recognized as important class of light-weight material for aviation structures [17]. Inclusion of Cu to Al matrix showed enhanced strength, hardness, machinability, less wear and fatigue. However, there was limited literature reported on Al/Cu functionally graded material. Thus, present work deals with the development of Al/Cu FGM via powder metallurgy process and understand its microstructure and mechanical behavior. Furthermore, the demand for FGMs in tribo-elements like piston rings and bearings is increasing rapidly [18–20]. Hence, it is essential to understand the tribological behavior of Al/Cu FGM. Thus, current research presents the friction and wear characteristics of FGM along with mechanical behavior for its wider usage in industrial applications.

Experimentation procedures

Raw materials

Raw materials utilized for experimentation work are aluminum (Al) and copper (Cu) metal powders of 99.9% purity as supplied by SRL Chemicals, India. Average particle size for both the raw materials is 44 µm. SEM micrographs shown in Fig. 1a and Fig. 1b reveal the morphology of Al as semi-spherical and Cu as dendritic.

Preparation of Al/Cu functionally graded sample

As illustrated in Fig. 2a, the FGM sample is designed to have five layers with varying weight fraction of constituents at the intermediate layers. While, extreme layers comprise base materials. Specimens were fabricated using a powder metallurgical die having a volume of $30 \times 10 \times 10\,mm^3$. Thickness of individual layer is maintained as 2 mm each. According to weight percentage, the raw materials at each layer were blended separately in a planetary ball mill for 1 hr. to obtain uniform mixture. Premixed constituents were then infused in a die from bottom layer to the top, followed by compaction using a hydraulic press. The compacted green specimen shown in Fig. 2b was sintered in a muffle furnace at 630 °C [17,21] for 2 hr. For comparison, base materials of pure aluminum and copper samples were fabricated in the same die using powder metallurgy.

Sample preparation

Sample preparation of metallographic specimens was essential to determine the microstructure accurately. Test specimens often undergo sectioning, coarse to fine grinding, polishing, and followed by etching. Using optical microscopy, the microscopic examination was performed at a magnification of 200 µm and advanced examination was done using SEM.

Micro hardness test

Hardness of Al/Cu FGM sample was observed Micro Vickers hardness tester having a diamond indenter. Indentation is of a right pyramid, wherein the hardness number (HV) was evaluated by Eq. 1.

$$HV = 0.1891\frac{P}{d^2}; d = \frac{h + v}{2} \quad (1)$$

Here P denote load (N), d signify diagonal of square impression (mm) and h & v represent horizontal & vertical lengths (mm).

Compressive strength test

Following ASTM D695 standards, compressive strength of Al/Cu FGM, pure Al, and pure Cu samples was performed on Universal Testing Machine (UTM) with a crosshead speed of 5 mm/min. Experiments were carried out at room temperature.

Sliding wear experimentation

Un-lubricated sliding wear experiments were performed on pin-on-disc tribometer depicted in Fig. 3, as supplied by DUCOM. Wear behavior was studied at different experimental conditions like normal loading (10, 20, 30 & 40 N), sliding velocity (1, 2, 3 & 4 m/s) and sliding distance (500, 1000, 1500 & 2000 m) maintaining constant atmospheric conditions (30 °C). Testing was performed according to ASTM G99 standards on a rectangular pin (30 mm height and 10 mm thickness) pressed against EN 31 hardened steel counter surface. LVDT sensors measure the frictional force, wear, and coefficient of friction (µ) which were obtained from WINDUCOM software. Using acetone, interacting surfaces were cleaned before and after each experimentation to remove wear debris which could affect the test results. Specific wear rate (in cm^3/Nm) was estimated using formula $\triangle w/F_n \rho L$, here $\triangle w$ represent mass loss (in g) measured by analytical balance, F_n is normal load (in N), ρ signify the density of pin (in g/cm^3) and L is sliding distance (in m). Five identical tests at each experimental condition was performed to obtain average results. Worn-out samples were observed under SEM to reveal dominant wear mechanisms and tribo-interactions that influence the abrasive wear.

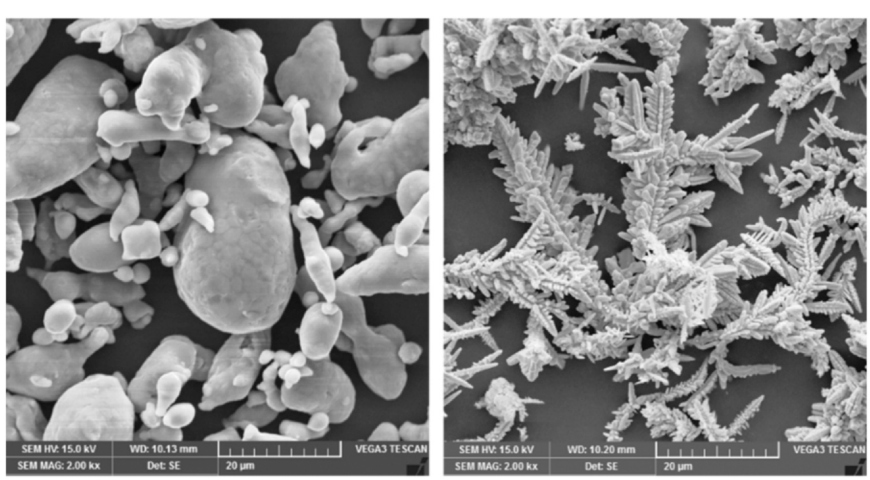

(a) (b)

Fig. 1. (a)-(b) SEM micrographs of Al and Cu particles.

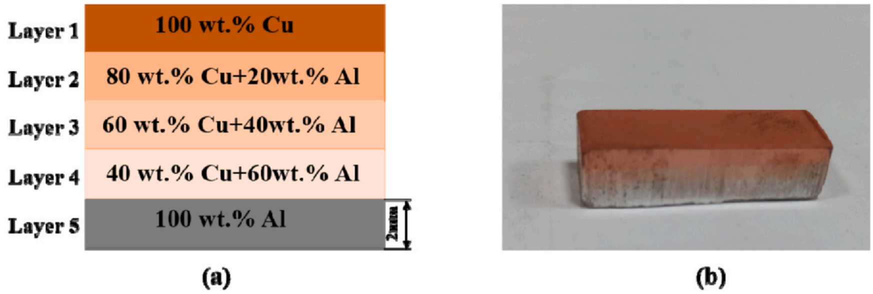

Fig. 2. (a) Design of five layered Al/Cu FGM (b) Green specimen.

Results and discussions

Metallographic study on Al/Cu FGM

After sample preparation, the microstructure was observed on a mirror polished specimen under an optical microscope. Fig. 4 shows the microstructure of FGM sample taken at the mid thickness of each layer to ensure the homogeneity of phase distribution. Microstructures reveal the presence of aluminum (in dark phase) and intermetallic compound of $CuAl_2$ (in bright phase). Formation of $CuAl_2$ phase at intermediate layers decrease with a decrease in copper content. Among all the layers, layer 2 showed most graded crystals of $CuAl_2$ due to the presence of high volume fraction of Cu phase. At the extreme layers 1 &5, only few crystals of $CuAl_2$ were noticed. With a decrease in volume fraction of Cu, distribution of intermetallic phase was decreased. But its morphology remains constant due to the fact that all the graded layers of the sample have undergone similar heating and cooling rates during sintering process. The intermetallic phase may significantly affect the mechanical behavior of Al/Cu FGM. Few research works on different FGMs cited in the references [10,22–24] reported the similar microstructural variation at graded layers. Formation of $CuAl_2$ is confirmed from XRD analysis shown in Fig. 5. Besides, trace amounts of cuprite (Cu_2O) were also found in the sample. This may be due to the existence of oxygen as one of the impurities in the raw copper powder which resulted in cuprite formation during sintering. In FGM sample cracks were not seen at the layers or on the interface between individual layers indicating the strong bonding among graded layers. Sintering causes the strong bonding among Cu and Al particles present at the different layers of compacted specimen. During this process, the individual particle morphologies disappear and the material forms as a mass. Additionally, the porosity is also reduced during sintering. The main mechanism responsible for strong bonding is diffusion that occurs during sintering stage. During diffusion, the distance between Al and Cu particles reduce, and the material is being transported within each layer of FGM resulting in strong bonding between the layers.

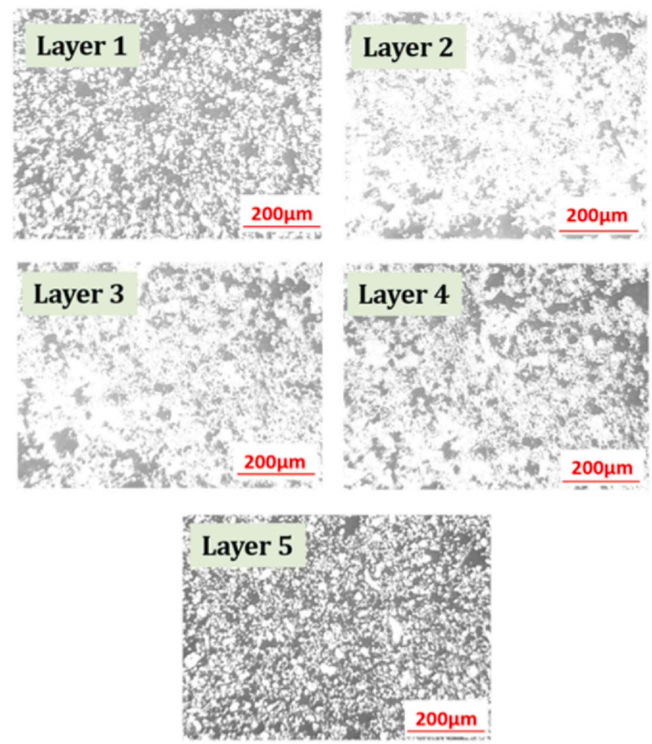

Fig. 4. Microstructure variation in Al/Cu FGM sample.

Hardness of Al/Cu functionally graded sample

Presence of gradation along thickness direction, FGM sample exhibited a varied hardness at different layers as shown in Fig. 6. At layers 1 and 5, due to the presence of pure copper and aluminum, they exhibited a hardness of 42.2HV and 34.3HV, respectively. The intermediate layers graded with both Al and Cu showed greater hardness compared to extreme layers. With a decrement in copper weight

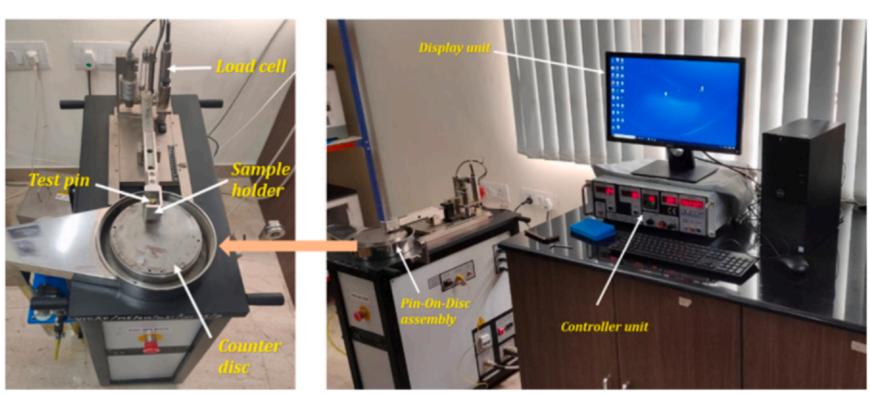

Fig. 3. Pin-On-Disc tribometer.

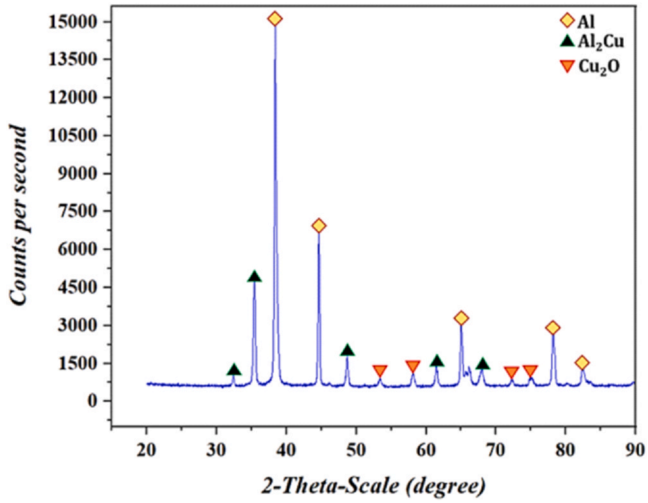

Fig. 5. XRD analysis of Al/Cu FGM sample.

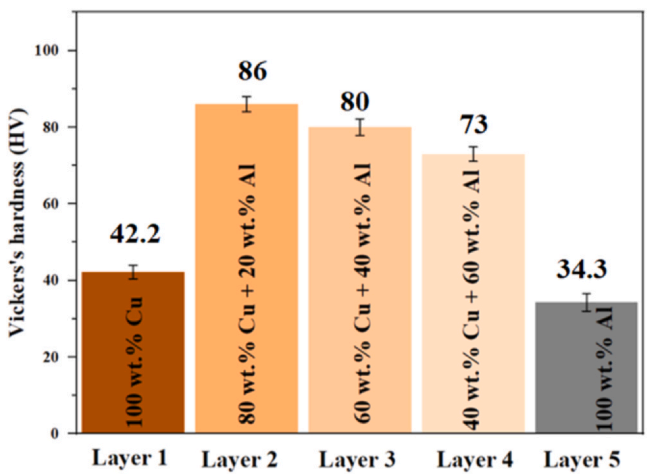

Fig. 6. Hardness at individual layers of Al-Cu FGM.

percentage, the hardness decreased from 86HV to 73HV from layer 2 to layer 4. At graded region, copper aluminide ($CuAl_2$) formed as intermetallic compound which enhance the hardness. Besides, $CuAl_2$ exhibit greater hardness and density than α-Al phase and thus graded layers showed improved hardness.

Compressive strength of base materials and FGM

The results indicated in Fig. 7 shows the compressive strength of pure Al, pure Cu and FGM specimens experienced compressive loading at room temperature. Pure copper was harder and more ductile than aluminum, it exhibits high strength. Its strength was 23.52% higher compared to pure Al sample. Strengthening of base materials was observed when they graded as functionally graded materials. Al/Cu FGM showed 40.9% and 22.7% greater compressive strength compared to raw Al and Cu samples, respectively. Increase in compressive strength may be due to distribution of fractured Cu particles in the Al matrix which arrests their dislocation movement. Besides, formation of Al_2Cu phase results in improvement of hardness and provides resistance to compressive load. In FGM, Cu was considered as reinforcement owing to its high strength compared to Al. During crack propagations, interfacial layers' act as crack arresters wherein crack deviation occurs and further propagation gets hindered [25,26]. The quality of bonding and interfaces strongly depend on fabrication process. In the present work, as PM technique was adopted which resulted in strong bonding among the graded layers which improved the compressive strength of FGM.

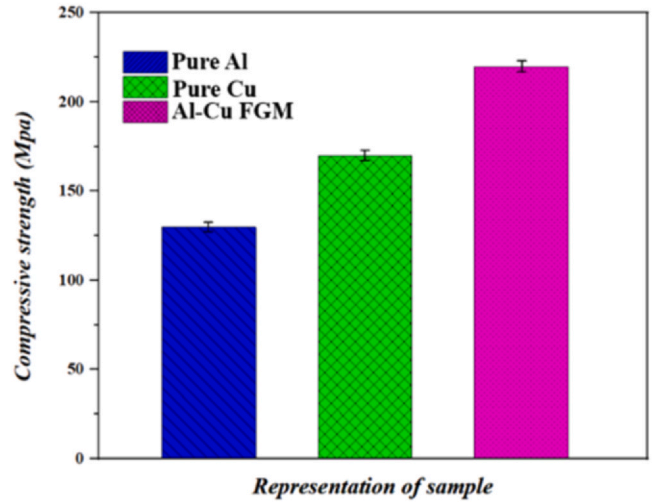

Fig. 7. Compressive strength of pure Al, Cu and FGM specimens.

Fractography of failure FGM specimens was observed through SEM at different magnifications after performing the compressive test. Ductile fracture was likely to be observed due to deformable nature of constituent elements. Presence of many dimples with varied sizes was seen from micrograph Fig. 8a. Additionally, cracks were also visible from Fig. 8b, which may occur due to detachment of interfacial layers under compressive loading. These observations were in good agreement with the research cited in references [27–30]. Also, graded layers show ductile fracture mechanism due to the presence of both Al and Cu. Unlike traditional composites and alloys [26,31], FGMs composed of fewer voids as shown in the Fig. 8c due to gradation in the specimens. Increase in Cu content result in enhancement of ductility which reduced the voids.

Sliding wear behavior of Al/Cu functionally graded material

Effect of applied load on sliding wear of Al/Cu FGM, pure Al and pure Cu is illustrated in Fig. 9a. Following Archard's law, wear rate shows a linear variation with the applied normal load from 10 N to 40 N and it was less significant in FGM compared to base materials. At 10 N loading condition, specific wear rate of FGM was lower due to work hardening behavior of graded layers. There exists a homogeneous load transfer among the elements present at layers which develops the softer wear debris. These debris act like a lubricating layer and decrease the wear rate. In addition, formation of thin cuprous oxide layer on FGM sample promoted mild wear at lower load. When load was increased to 40 N, high stresses were induced at the contact of sample and counter surface. Due to which oxide layer was completely removed and cracks were propagated resulting in higher wear. The counter surface material got penetrated in to the subsurface layers of FGM, causing severe plastic deformation at higher load condition. Similar wear behavior was observed in Cu-WC functionally graded composite as cited in reference [32]. Thus, dominant wear mechanisms at lower load were identified as abrasive. While, adhesive and delamination was observed at greater loading conditions. At 10 N, 1 m/s and 500 m sliding distance, the wear rate of FGM was 47.8% and 29.6% lower than pure Al and pure Cu respectively.

Influence of sliding velocity on specific wear rate of FGM and base materials was evaluated by applying a constant load and sliding distance of 30 N and 500 m respectively. Decrement in wear rate with an increase in sliding velocity was observed from Fig. 9b. Nearly 52.9% reduction in wear rate was observed with functionally graded sample as velocity increased from 1 m/s to 4 m/s. During experimentation, Al and Cu particles break into the powder creating voids on the sample surface. These voids were filled with the wear debris that form as lubricating

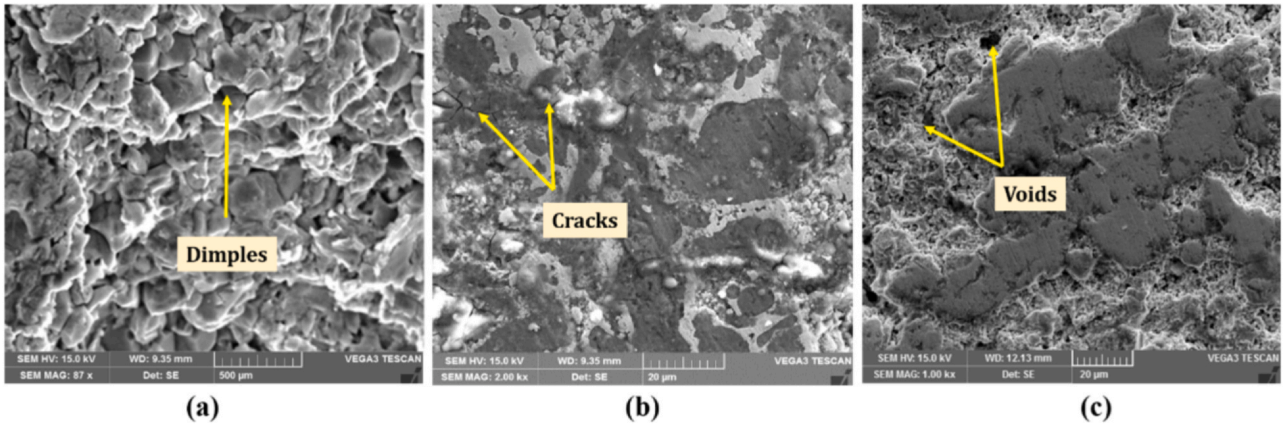

Fig. 8. (a)-(c) SEM micrographs showing the failure mechanisms in Al-Cu FGM sample.

layer to decrease friction and wear. At 4 m/s speed, initial wear of samples was more which results in greater material removal. These particles act as soft wear debris which were accumulated on the counter disc. As disc rotates at high velocity, the wear debris were pushed out of the track due to centrifugal force resulting in less wear rate [33,34]. At low sliding velocity of 1 m/s, pin shows a direct contact with the counter disc for sufficient time to induce temperature, which in turn increase the wear. While, at higher sliding speeds, interfacial surfaces heat up faster and material tend to flow over counter disc to lower the abrasive wear.

At constant sliding velocity of 1 m/s and applied normal load of 20 N, wear rate was studied by varying the sliding distances from 500 m to 2000 m. All the test samples showed an increase in wear rate up to

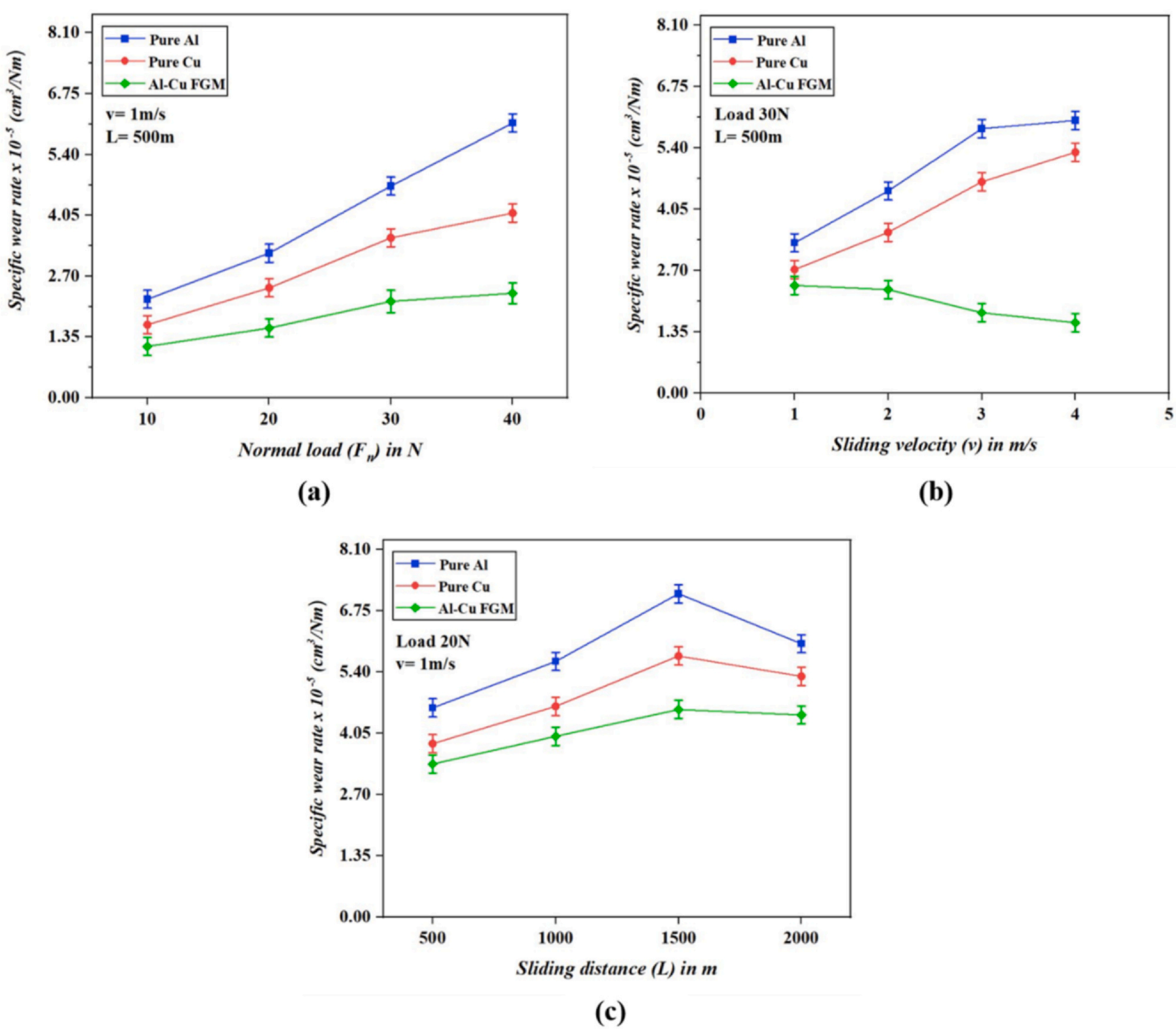

Fig. 9. (a)-(c) Effect of load, sliding velocity and sliding distance on specific wear rate.

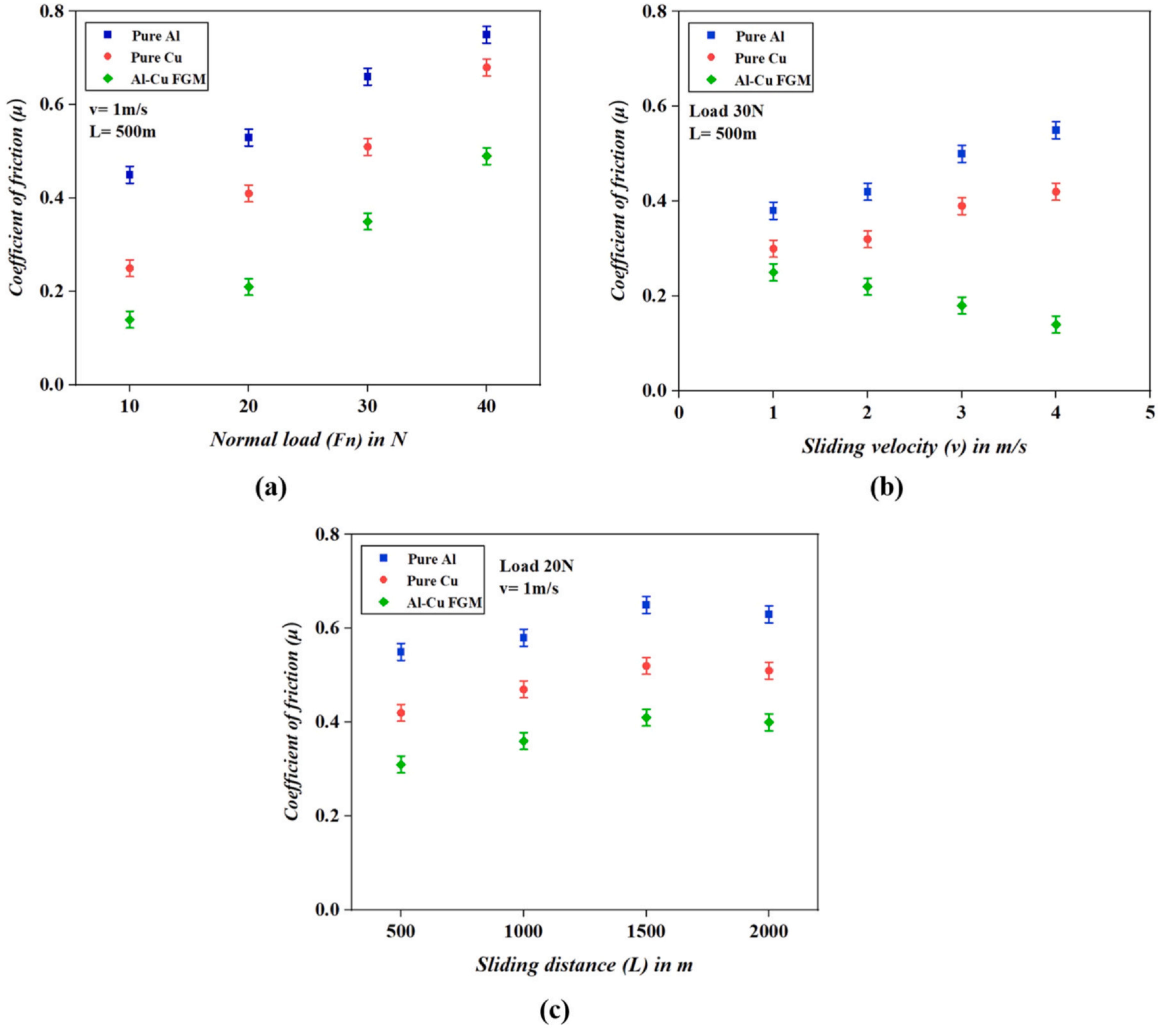

Fig. 10. (a)-(c) Effect of load, sliding velocity and sliding distance on frictional coefficient.

sliding distance of 1500 m and beyond which marginal decrement was noticed from Fig. 9 c. A 2.62% reduction in wear rate from 1500 m to 2000 m sliding distance was seen in case of FGM sample. Due to plastic deformation, some amount of material from test sample was removed as asperities. These hard asperities interact with the counter surface which results in high wear rate. With an increase in sliding distance, more wear debris accumulate into cavities created by broken particles and protect the sample from further wear-off. Thus, 1500 m was considered as critical limit of sliding distance to promote wear resistance. Moreover, samples heat up because of frictional heating at higher sliding distance [35,36]. Wear rate of FGM was observed to be lower in all testing conditions was due to the presence of high amount of wear debris at interacting surfaces that reduce effective contact area. After sliding distance of 1500 m, wear resistance of pure Al was decreased compared to pure Cu. This can be due to the formation of oxide layers of Al_2O_3 and Cu_2O on pure Al and pure Cu samples respectively. During sliding experiment, temperature is increased at contact zone due to the friction and the pin material absorbs heat generated at the interface. As thermal conductivity of Al_2O_3 is being more than Cu_2O, more heat was absorbed by the pure Al and thus resulted in high wear rate.

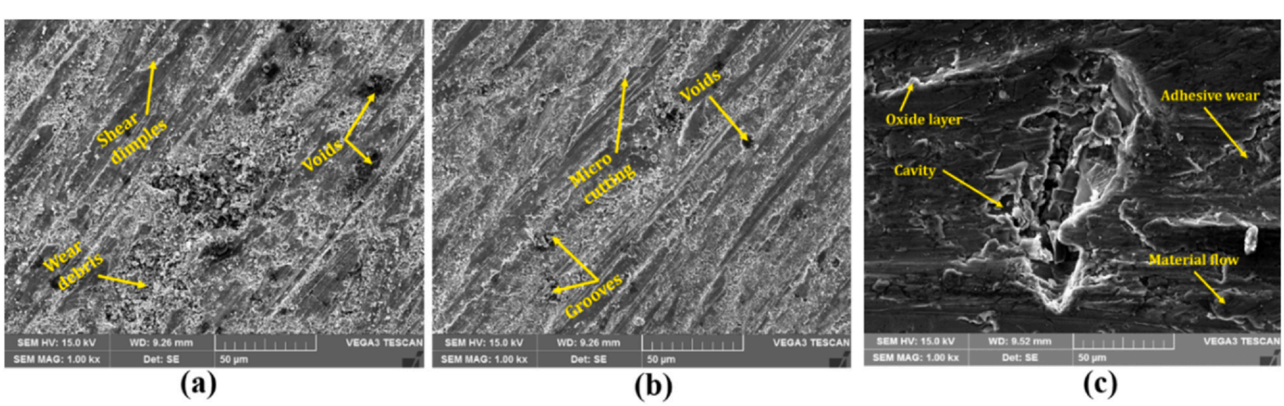

Fig. 11. (a)-(c) Worn surfaces of pure aluminum, pure copper and Al/Cu FGM at 40 N loading.

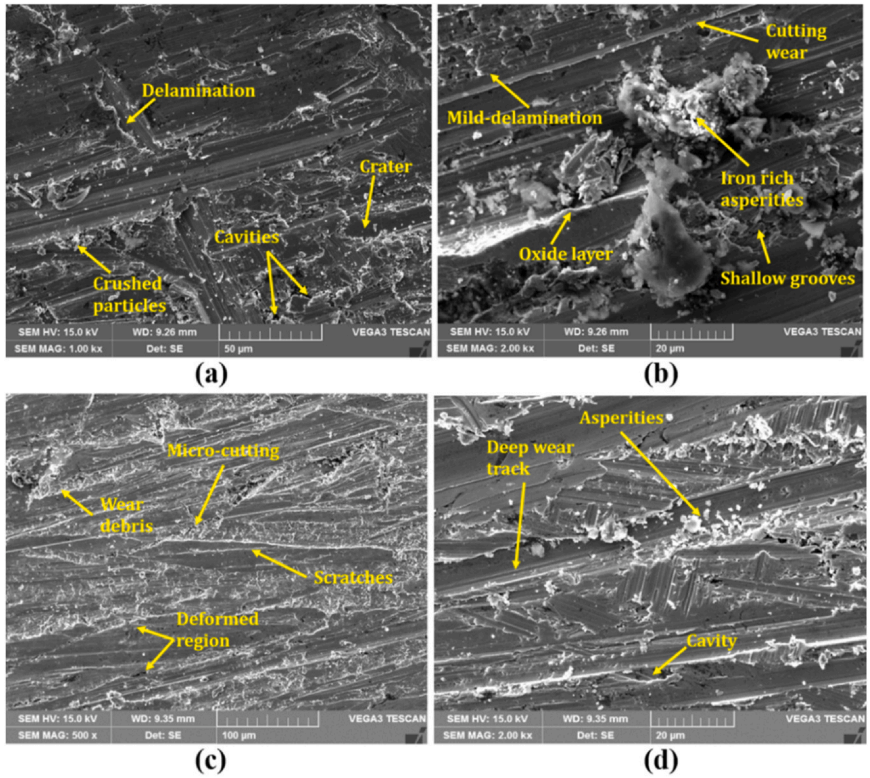

Fig. 12. (a)-(d) Worn surfaces of FGM at low and high sliding velocity and sliding distance conditions.

Coefficient of friction (COF) of Al/Cu functionally graded material

Frictional coefficient shows a direct proportionality with regard to applied normal load for all the samples as illustrated in Fig. 10a. With an increase in normal load, the contact area between pin and counter disc surfaces reduces, resulting in greater material loss. Presence of more asperities that cause abrasion to sample surface decrease the wear resistance thereby increase the friction. COF of FGM at 40 N was 53% and 38.7% less than pure Al and pure Cu respectively. Coefficient of friction as a function of sliding velocity was shown in Fig. 10b. Functionally graded sample exhibited decrement in friction with an increase in sliding velocity from 1 m/s to 4 m/s. This is due to the increase in shear and bulk deformation along with work hardening which reduce the contact area between FGM and disc surfaces, thereby friction decreases. Compared to lower velocity, wear debris causing abrasion were blown away from the counter surface by centrifugal forces at higher speeds. On the contrary, friction and wear increase with an increase in sliding velocity for base materials due to three body abrasion.

Effect of sliding distance on COF was observed from Fig. 10c reveals the increase in friction up to 1500 m sliding distance beyond that a marginal decrement was observed. This decrease in friction was due to thermal softening phenomenon and tribo layer formation at the contact of pin and counter surface. Small variation in friction indicates the presence of less defects (or) cracks on the surface which could affect the frictional coefficient. Samples lost their resistance towards deformation adhesion when sliding distance increased from 500 m to 1500 m, thus, resulting in more friction [37].

Worn-out surface examination

The surface of worn-out samples after sliding wear test under different loading, sliding velocity and sliding distance conditions were observed using SEM to study dominant wear mechanisms. When the base materials slide against EN 31 hardened steel counter disc, micro cracking and delamination were seen at lower load of 10 N maintaining constant sliding velocity and distance. When the applied load increased to 40 N, sharp asperities accumulate on the disc and penetrate in to sample surface resulting in greater material loss. Wear features like deep grooves, micro-cutting and shear dimples illustrated in Fig. 11a and Fig. 11b were evident on worn surface of pure Al and pure Cu respectively. In contrast, different wear characteristics were observed on worn surface of FGM. Presence of less grooves at low and high loading indicate smoother surface which reduce friction and wear as compared to base materials. One more reason was the formation of oxide layer (OL) or mechanically mixed layer shown in Fig. 11c promote wear resistance. The OL in FGM was confirmed through EDX and XRD analysis discussed in Section 3.2. The oxide layer reduces wear and friction by 50.8% and 71.4% of FGM with an increase in load from 10 N to 40 N. Study on Al alloy/SiC composites reported by Gul and Acilar [38] observed similar oxide layer formation in lowering the friction. Wear mechanism in FGM was identified as adhesive due to inadequate grooves and wear occurs by material flow. While, surface of base materials reveals abrasive wear initiated by plowing of soft material by hard asperities. Due to low ductile nature of Al, more particles were removed as wear debris resulting in high wear compared to pure Cu.

The trend of wear and friction in the case of FGM decrease with an increase in sliding speed from 1 m/s to 4 m/s. At the velocities above 2 m/s, thermal stability of sample increases due to high hardness of intermetallic compound of copper aluminide ($CuAl_2$). Increase in sliding velocity promote the flow strength and strain rate of sliding surface. As a result, contact area reduces and lower the friction and wear. During the initial sliding condition, metal to metal contact was established and hard asperities from counter surface remove the soft aluminum particles from the sample. Owing to high hardness of $CuAl_2$ particles compared to steel, they remove the iron particles from the disc surface by scratching. During this time, some of the intermetallic particle's fragment under applied pressure to form wear debris along with other asperities. On further sliding, debris present at the interface was crushed into finer size and from a lubricating layer. At higher speeds, few wear debris were transferred into sliding contacts to fill the cavities/voids formed by broken particles. And some debris were pushed away from the interface due to greater centrifugal forces. As metallic contact was reduced between sliding surfaces, friction and wear reduce due to decreased adhesion.

Wear mechanism at low sliding velocity was identified by cavities and craters represented in Fig. 12a. While, micro cutting, mild delamination and oxidation was observed at sliding velocity of 4 m/s (see Fig. 12b). Similar wear mechanisms were shown by Cu/MoS_2 composites fabricated through powder metallurgy [39]. In the case of pure Al and Cu, more metallic contact was established which weakens the subsurface due to high temperature occurrence in sliding condition. Besides, presence of no intermetallic phase cause severe plastic deformation and delamination in base materials. Worn out surface of FGM at lower and higher sliding distances of 500 m and 1500 m shows minor scratches and deep wear tracks respectively as illustrated in Fig. 12c and Fig. 12d. Formation of intermetallic compound and OL reduced the severity of abrasive wear in functionally graded material in all sliding conditions.

Conclusions

In the current research, Al/Cu functionally graded material (FGM) was fabricated using powder metallurgy. Based on the experiments, the following results were presented.

- FGM showed a variation in microstructure along thickness direction due to gradation of materials. EDS and XRD analysis reveal the formation of cuprous oxide (Cu_2O) layer and intermetallic phase of copper aluminide ($CuAl_2$).
- During sintering, copper gets dissolved in Al matrix to form solid solution with an increase in temperature. While cooling down, $CuAl_2$ precipitated from Al and its content increased at the graded layers. As a result, FGM sample showed greater hardness at intermediate layers.
- Compressive strength of Al/Cu FGM was 40.9% and 22.7% greater compared to pure Al & pure Cu samples, respectively. A strong interfacial bonding among graded layers hinder the crack propagation, in turn improved the strength. Furthermore, ductile failure was observed from SEM micrographs which reveal the formation of dimples, cracks, and fewer voids.
- In sliding wear behavior, FGM showed superior wear resistance compared to base materials. Increase in wear rate and COF was observed with an increase in normal load. More stresses were induced at higher loading which results in crack formation and propagation, leading to greater wear.
- Under the influence of sliding velocity with constant normal load, wear rate and COF of FGM decrease as velocity increase from 1 m/s to 4 m/s. Centrifugal forces at higher speed push away the asperities causing abrasion from counter surface to reduce the wear. Nearly 52.9% and 44% reduction in wear rate and COF was observed in functionally graded sample as velocity increased from 1 m/s to 4 m/s.
- Test specimens showed increased wear rate up to critical sliding distance, beyond which a marginal decrement was observed. With an increase in sliding distance, more wear debris were accumulated into the sites created by broken particles and protect the samples from further wear-off.
- Worn out surface analysed through SEM reveals the presence of shear dimples, voids, wear asperities, cracks, and grooves on the pure Al and Cu materials. And mild delamination, fewer voids/cavities and oxide layer formation was found on FGM.

Declaration of Competing Interest

The authors declare that they have no known competing financial interests or personal relationships that could have appeared to influence the work reported in this paper.

References

[1] V. Boggarapu, R. Gujjala, S. Ojha, S. Acharya, V.B. Peddakondigalla, S. Chowdary, Kumar, D. Gara, State of the art in functionally graded materials, Compos. Struct. 262 (2021) 113596, https://doi.org/10.1016/j.compstruct.2021.113596

[2] H. Ahmadian, A.M. Sadoun, A. Fathy, T. Zhou, Utilizing a unified conceptual dynamic model for prediction of particle size of duel-matrix nanocomposites during mechanical alloying, Powder Technol. 418 (2023) 118291, https://doi.org/10.1016/j.powtec.2023.118291

[3] A.M. Sadoun, F. Abd El-Wadoud, A. Fathy, A.M. Kabeel, A.A. Megahed, Effect of through-the-thickness position of aluminum wire mesh on the mechanical properties of GFRP/Al hybrid composites, J. Mater. Res. Technol. 15 (2021) 500–510, https://doi.org/10.1016/j.jmrt.2021.08.026

[4] A.M. Sadoun, A.F. Meselhy, A.W. Deabs, Improved strength and ductility of friction stir tailor-welded blanks of base metal AA2024 reinforced with interlayer strip of AA7075, Results Phys. 16 (2020) 102911, https://doi.org/10.1016/j.rinp.2019.102911

[5] V. Boggarapu, S. Adapa, R. Kanakam, S. Ojha, R. Gujjala, Research on mechanical and erosion behavior of stepped polymeric functionally graded materials reinforced with aluminum, Polym. Compos. 43 (2021) 1048–1059 doi.org/10.1002/pc.26433.

[6] M. Naebe, K. Shirvanimoghaddam, Functionally graded materials: a review of fabrication and properties, Appl. Mater. Today 5 (2016) 223–245, https://doi.org/10.1016/j.apmt.2016.10.001

[7] B. Saleh, J. Jiang, R. Fathi, T. Al-hababi, Q. Xu, L. Wang, D. Song, A. Ma, 30 Years of functionally graded materials: an overview of manufacturing methods, Appl. Future Chall. Compos. B Eng. 201 (2020) 108376, https://doi.org/10.1016/j.compositesb.2020.108376

[8] V. Boggarapu, L. Ruthik, D.K. Gara, S. Ojha, S. Jain, R. Gujjala, A.K. Bandaru, R. Inala, Study on mechanical and tribological characteristics of layered functionally graded polymer composite materials, Proc. Inst. Mech. Eng. E. J. Process. Mech. Eng. 236 (2022) 1857–1868, https://doi.org/10.1177/09544089221074841

[9] Q. Cong, F. Xu, Y. Tan, X. Shi, W. Dong, J. Li, J. Zhang, Influence of heat treatment on microstructure and mechanical properties of Al/Al-Cu graded materials, Acta Metall. Sin. Engl. Lett. 24 (2011) 118–124, https://doi.org/10.11890/1006-7191-112-118

[10] F.M. Xu, S.J. Zhu, J. Zhao, M. Qi, F.G. Wang, S.X. Li, Z.G. Wang, Effect of stress ratio on fatigue crack propagation in a functionally graded metal matrix composite, Compos. Sci. Technol. 64 (2004) 1795–1803, https://doi.org/10.1016/j.compscitech.2004.01.009

[11] J. Zhu, Z. Lai, Z. Yin, J. Jeon, S. Lee, Fabrication of ZrO2–NiCr functionally graded material by powder metallurgy, Mater. Chem. Phy. 68 (2001) 130–135, https://doi.org/10.1016/S0254-0584(00)00355-2

[12] H. Kwon, C.R. Bradbury, M. Leparoux, Fabrication of functionally graded carbon nanotube-reinforced aluminum matrix composite, Adv. Eng. Mater. 13 (2011) 325–329, https://doi.org/10.1002/adem.201000251

[13] G. Kırmızı, H. Arık, H. Çinici, Experimental study on mechanical and ballistic behaviours of silicon carbide reinforced functionally graded aluminum foam composites, Compos. B Eng. 164 (2019) 345–357, https://doi.org/10.1016/j.compositesb.2018.11.076

[14] F.F. Kamaruzaman, D.M. Nuruzzaman, M.A. Chowdhury, S.N.S. Jamaludin, S. Basri, N.M. Ismail, Characterisation of four-layered Al-Al2O3 functionally graded material prepared through powder metallurgy and pressureless sintering, Int. J. Mater. Prod. Tecnol. 59 (2019) 48–62, https://doi.org/10.1504/IJMPT.2019.100832

[15] G.S. Alsoruji, A.M. Sadoun, M. Abd Elaziz, M.A. Al-Betar, A.W. Abdallah, A. Fathy, On the prediction of the mechanical properties of ultrafine grain Al-TiO2 nanocomposites using a modified long-short term memory model with beluga whale optimizer, J. Mater. Res. Technol. 23 (2023) 4075–4088, https://doi.org/10.1016/j.jmrt.2023.01.212

[16] I. Najjar, A. Sadoun, M.N. Alam, A. Fathy, Prediction of wear rates of Al-TiO2 nanocomposites using artificial neural network modified with particle swarm optimization algorithm, Mater. Today Commun. 35 (2023) 105743, https://doi.org/10.1016/j.mtcomm.2023.105743

[17] V. Boggarapu, P.S. Rama Sreekanth, V.B. Peddakondigalla, P.P. Parvathaneni, S. Ojha, J. Gujjala, S. Jain, Babu Valasingam, Gujjala R, Experimental study on tribological behavior of aluminum–copper functionally graded material, Proc. Inst. Mech. Eng. L J. Mater. Des. Appl. 237 (2023) 1592–1602, https://doi.org/10.1177/14644207221150095

[18] I. Najjar, A. Sadoun, A. Fathy, On the understanding and prediction of tribological properties of Al-TiO2 nanocomposites using artificial neural network, J. Compos. Mater. 57 (2023) 2325–2337, https://doi.org/10.1177/00219983231171690

[19] V. Boggarapu, R. Gujjala, S. Ojha, A critical review on erosion wear characteristics of polymer matrix composites, Mater. Res. Express 7 (2020) 022002, https://doi.org/10.1088/2053-1591/ab6e7b

[20] A.M. Sadou, A.F. Meselhy, A.W. Abdallah, Microstructural, mechanical and wear behavior of electroless assisted silver coated Al2O3–Cu nanocomposites, Mater. Chem. Phy. 266 (2021) 124562, https://doi.org/10.1016/j.matchemphys.2021.124562

[21] M.M. Nemat-Alla, M.H. Ata, M.R. Bayoumi, W. Khair-Eldeen, Powder metallurgical fabrication and microstructural investigations of aluminum/steel functionally graded material, Mater. Sci. Appl. 2 (2011) 1708–1718, https://doi.org/10.4236/msa.2011.212228

[22] K. Rajasekhar, V.S. Babu, M.J. Davidson, Microstructural and mechanical properties of Al-Cu functionally graded materials fabricated by powder metallurgy method, Mater. Today Proc. 41 (2021) 1156–1159, https://doi.org/10.1016/j.matpr.2020.09.157

[23] V. Boggarapu, P.S. Rama Sreekanth, V.B. Peddakondigalla, S.C. Mallampati, R. Kanakam, S. Ojha, J. Gujjala, S.B. Valasingam, R. Gujjala, A novel approach to develop and characterize bi-directional aluminum-copper functionally graded material, 09544089231163746, Proc. Inst. Mech. Eng. E. J. Process. Mech. Eng. (2023), https://doi.org/10.1177/14644207221150095

[24] Y. Watanabe, Y. Hattori, H. Sato, Distribution of microstructure and cooling rate in Al–Al2Cu functionally graded materials fabricated by a centrifugal method, J. Mater. Proc. Technol. 221 (2015) 197–204, https://doi.org/10.1016/j.jmatprotec.2015.01.0280
[25] P. Mardiha, A. Bahrami, A. Mohammadnejad, Towards a high strength ductile Ni/Ni3Al/Ni multilayer composite using spark plasma sintering, Sci. Sinter. 51 (2019) 401–408, https://doi.org/10.2298/SOS1904401M
[26] P. Mardiha, A. Bahrami, A. Mohammadnejad, An investigation on the microstructure, interface, and mechanical properties of spark plasma sintered Ni/Ni-Ni3Al/Ni compound, J. Mater. Eng. Perform. 31 (2022) 1163–1169, https://doi.org/10.1007/s11665-021-06227-9
[27] M. Tayyebi, M. Alizadeh, A novel two-step method for producing Al/Cu functionally graded metal matrix composite, J. Alloy. Compd. 911 (2022) 165078 ,https://doi.org/10.1016/j.jallcom.2022.165078
[28] Y. Zhao, K. Liu, H. Hou, L.Q. Chen, Role of interfacial energy anisotropy in dendrite orientation in Al-Zn alloys: a phase field study, Mater. Des. 216 (2022) 110555, https://doi.org/10.1016/j.matdes.2022.110555
[29] V. Boggarapu, S. Jain, S. Ojha, A.K. Bandaru, R. Gujjala, Erosion wear characteristics of step-wise layered polymer composite materials by silica sand particles, Proc. Inst. Mech. Eng. L J. Mater. Des. Appl. 236 (2022) 2539–2549, https://doi.org/10.1177/14644207221100043
[30] V.Y. Mehr, M.R. Toroghinejad, A. Rezaeian, Mechanical properties and microstructure evolutions of multilayered Al–Cu composites produced by accumulative roll bonding process and subsequent annealing, Mater. Sci. Eng. A 601 (2014) 40–47, https://doi.org/10.1016/j.msea.2014.02.023
[31] A. Bahrami, A. Miroux, J. Sietsma, Modeling of strain hardening in the aluminum alloy AA6061, Met. Mater. Trans. A 44 (2013) 2409–2417, https://doi.org/10.1007/s11661-012-1594-6
[32] N. Radhika, R. Reghunath, M. Sam, Improvement of mechanical and tribological properties of centrifugally cast functionally graded copper for bearing applications, Proc. Inst. Mech. Eng. L J. Mech. Eng. Sci. 233 (2019) 3208–3219, https://doi.org/10.1177/0954406218805508
[33] C.H. Sri Chaitanya, R. Narasimha Rao, Tribological behavior of cenosphere-filled epoxy syntactic foams in dry sliding conditions, J. Tribol. 142 (2020) 051701, https://doi.org/10.1115/1.4045768
[34] A. Sadoun, A. Ibrahim, A.W. Abdallah, Fabrication and evaluation of tribological properties of Al2O3 coated Ag reinforced copper matrix nanocomposite by mechanical alloying (doi.org/), J. Asian Ceram. Soc. 8 (2020) 1228–1238, https://doi.org/10.1080/21870764.2020.1841073
[35] N. Radhika, J. Sasikumar, J.L. Sylesh, R. Kishore, Dry reciprocating wear and frictional behaviour of B4C reinforced functionally graded and homogenous aluminium matrix composites, J. Mater. Res. Technol.. 9 (2020) 1578–1592, https://doi.org/10.1016/j.jmrt.2019.11.084
[36] A. Mohamed, M.M. Mohammed, A.F. Ibrahim, O.A. El-Kady, Effect of nano Al2O3 coated Ag reinforced Cu matrix nanocomposites on mechanical and tribological behavior synthesis by P/M technique, J. Compos. Mater. 54 (2020) 4921–4928, https://doi.org/10.1177/0021998320934860
[37] P.L. Menezes, S.V. Kailas, Role of surface texture of harder surface on subsurface deformation, Wear 266 (2009) 103–109, https://doi.org/10.1016/j.wear.2008.05.008
[38] F. Gul, M. Acilar, Effect of the reinforcement volume fraction on the dry sliding wear behaviour of Al–10Si/SiCp composites produced by vacuum infiltration technique, Compos. Sci. Technol. 64 (2004) 1959–1970, https://doi.org/10.1016/j.compscitech.2004.02.013
[39] P.S. Kumar, K. Manisekar, Prediction of effect of MoS2 content on wear behavior of sintered Cu-Sn composite using Taguchi analysis and artificial neural network, Indian J. Eng. Mater. Sci. 21 (2014) 657–671 nopr.niscpr.res.in/handle/123456789/30525.